A three-dimensional semi-analytical model for the prediction of underwater noise from offshore pile driving

Apostolos Tsouvalas, Andrei V. Metrikine
Delft University of Technology, Faculty of Civil Engineering and Geosciences, Section of Structural Mechanics, Stevinweg 1, 2628CN Delft, The Netherlands

Summary
In this study, a three-dimensional semi-analytical pile-water-soil interaction model is presented for the prediction of underwater noise from offshore pile driving. The pile is described by a thin shell theory and the hammer is substituted by a force applied at the head of the pile. The soil is modelled as three-dimensional elastic continuum and the water region is described by the linear acoustic wave equation. With the developed model, the wave radiation due to vibratory and impact pile driving is analysed. It is shown that the field generated by impact piling consists of powerful pressure conical fronts in the water column. In the soil region, both shear and compressional waves are generated, with the former being much stronger than the latter. Scholte waves are generated along the seabed-water interface, which induce low-frequency pressure fluctuations in the water column close to the seabed surface. The energy launched by the hammer into the water and into the soil is investigated for both hammer types in order to highlight the main differences regarding the generated wave field. The present work aims to provide the scientific and engineering community with an in-depth physical understanding of the main sources that can possibly contribute to the underwater noise associated with pile driving in offshore environments.

PACS no. xx.xx.Nn, xx.xx.Nn

1. Introduction

To meet today's increasing energy demand, a large number of offshore wind farms are planned for construction in the near future. Although several foundation concepts have been developed so far, in order to support the tower of offshore wind power generators, the most common of those is a steel monopile. Steel monopiles are driven into the sediment offshore with the help of large impact or vibratory hammers. During the piling process, the generated underwater noise levels are very high. Measurements indicate that the noise levels close to the pile due to the impact hammers can be in the order of 10^5Pa [1].

The high noise levels generated by marine piling have naturally drawn the attention of regulatory bodies and environmental organisations in several nations. Erbe [2] provides a brief overview of the restrictions that several governments have imposed to protect the environment from the high underwater noise levels induced by pile driving. In The Netherlands, pile driving is permitted only from the first of July till the end of December in order to avoid disturbance of the breeding season of the harbour porpoise. In the United Kingdom [3], a separate environmental assessment is required per project. The German Federal government, on the contrary, adopts certain sound level criteria. These have been set to 160 dB re 1 μPa s for the sound exposure level and to 190 dB re 1 μPa for the sound peak pressure level, both measured at a distance of 750m from the surface of the pile [4]. Similar regulations exist in several other countries worldwide. Despite the fact that there is yet no overall consensus upon the most appropriate way of quantifying the level of noise which can be harmful to marine species, all the involved parties recognise that certain actions need to be undertaken in order to protect the marine ecosystem. What needs to be mentioned at this point is that sound, in particular low frequency sound associated with marine piling operations, can *travel* long distances. Thus, regulations should ideally consider this *transboundary character* of the noise pollution [5]. Unfortunately, to date, each country strives for a strict application of the legislation within its territorial waters without recognising the need for the development of uniformly accepted agreements with its neighbouring nations.

As can be concluded from the above, the problem of underwater noise generated by pile driving is multidisciplinary in nature. Scientists of various backgrounds as well as international environmental organizations are strongly involved. On the one hand, acousticians and engineers are striving to develop methods and tools which accurately predict the sound field radiated by marine piling. On the other hand, biologists and marine specialists are trying to identify and quantify the extent of possible damage that marine piling causes to the aquatic environment. In between, governmental organisations and regulatory bodies impose certain regulations and restrictions in order to minimise the underwater noise pollution. In essence, the solution to the problem requires the combined effort of several specialists in order to quantify noise, to assess its negative environmental impact and to propose solutions to eliminate it. The focus in this study is on the first aspect mentioned above: the prediction of the noise that is generated by marine pile driving.

The structure of this paper is as follows. In section 2 a linear pile-water-soil model is presented and the solution approach is briefly discussed. In section 3, structure-borne wave radiation associated with impact piling and vibratory installation are discussed. Finally, section 4 summarises the most important findings of the present study.

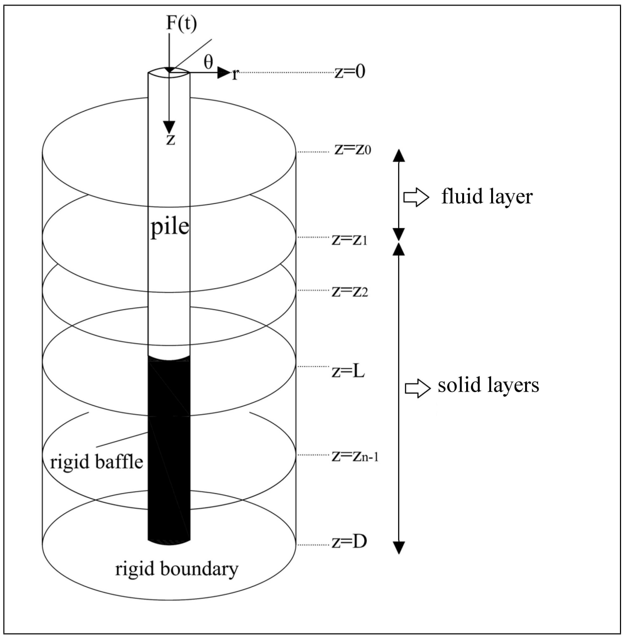

Figure 1. A schematic representation of a pile embedded into a layered medium. The fluid layer occupies the region $z_0 < z < z_1$ and $r > R$, whereas the solid layers are horizontally stratified in the region $z_1 < z < D$ and $r > R$. This model can be used for the prediction of the structure-borne wave radiation during the installation of a pile by an impact hammer or a vibratory device.

2. Pile-water-soil model

The total system consists of the shell and of the layered acousto-elastic domain as shown in Fig.1. The system is excited by a force applied at the top side of the shell. A linear high-order shell theory is considered for the description of the shell dynamics [6, 7]. The shell is of finite length and occupies the domain $0 \le z \le L$. The constants E, v, R, ρ and $2h$ correspond to the complex modulus of elasticity in the frequency domain, the Poisson ratio, the radius of the mid-surface of the shell, the density and the thickness of the shell respectively. The fluid is modelled as a three-dimensional inviscid compressible medium with a pressure release boundary at $z = z_0$ and occupies the domain $z_0 < z < z_1$ and $r > R$. The layered solid domain is described as a three-dimensional elastic continuum in $z_1 < z < D$ and $r > R$. The interface at $z = D$ is substituted by a rigid boundary. All layers are horizontally stratified and are distinguished by the index $j = 1, 2, ..., n$. The constants λ_j and G_j define the *Lamé* coefficients for each solid layer and ρ_j is the soil density. The various solid layers are in full contact with each other at the horizontal interfaces. At the interface with the fluid only the vertical stress equilibrium and the vertical displacement continuity are imposed (the shear stresses at the surface of the upper solid layer are set equal to zero). The shell structure is extended by a *rigid baffle* in the region $L < z < D$ to comply with the homogeneity of the domain along the $z-$coordinate at $r > R$. The following set of partial differential equations govern the linear dynamics of the coupled system in the frequency domain for the cylindrically symmetric case:

$$\begin{aligned}\mathbf{L}\tilde{\mathbf{u}}_p + \mathbf{I}_m \tilde{\mathbf{u}}_p = &- \left(H(z-z_1) - H(z-L)\right) \tilde{\mathbf{t}}_s \\ &+ \left(H(z-z_0) - H(z-z_1)\right) \tilde{\mathbf{p}}_f + \tilde{\mathbf{f}},\end{aligned} \tag{1}$$

$$G_j \nabla^2 \tilde{\mathbf{u}}_s^j + (\lambda_j + G_j) \nabla\nabla \cdot \tilde{\mathbf{u}}_s^j + \omega^2 \rho_j \tilde{\mathbf{u}}_s^j = \mathbf{0}, \tag{2}$$

$$\nabla^2 \tilde{\phi}_f(r,z,\omega) + \frac{\omega^2}{c_f^2} \tilde{\phi}_f(r,z,\omega) = 0. \tag{3}$$

In the equations above, $\tilde{\mathbf{u}}_p = \left[\tilde{u}_{p,z}(z,\omega)\, \tilde{u}_{p,r}(r,\omega)\right]^T$ is the displacement vector of the mid-surface of the shell, $\mathbf{u}_s^j(r,z,\omega) = \left(u_{s,z}^j(r,z,\omega),\, u_{s,r}^j(r,z,\omega)\right)^T$ is the displacement vector of each solid layer and $\tilde{\phi}_f(r,z,\omega)$ is a velocity potential introduced for the description of the fluid layer. The subscripts s and f correspond to the solid and the fluid, respectively. The operators $\mathbf{L}$ and $\mathbf{I}_m$ are the stiffness and modified inertia matrices of the shell, respectively [7]. The term $\tilde{\mathbf{p}}_f$ represents the fluid pressure exerted at the outer surface of the shell at $z_0 < z < z_1$. The functions $H(z - z_i)$ are the Heaviside step functions which are used here to account for the fact that the soil and the fluid are in contact with different segments of the shell. The vector $\tilde{\mathbf{f}} = \left[\tilde{f}_{rz}(z,\omega)\ \tilde{f}_{rr}(z,\omega)\right]^T$ represents the externally applied force on the surface of the shell. The term $\tilde{\mathbf{t}}_s$ represents the boundary stress vector that takes into account the reaction of the soil surrounding the shell at $z_1 < z < L$, i.e.

$$\tilde{\mathbf{t}}_s^j = \lambda_j \nabla \cdot \tilde{\mathbf{u}}_s^j \mathbf{I} + G_j \left(\nabla \tilde{\mathbf{u}}_s^j + \left(\nabla \tilde{\mathbf{u}}_s^j \right)^T \right), \quad (4)$$

in which j is used here to distinguish between the layers and $\mathbf{I}$ is the identity matrix. The Helmholtz decomposition is applied, i.e. $\tilde{\mathbf{u}}_s^j = \nabla \tilde{\phi}^j + \nabla \times \tilde{\boldsymbol{\psi}}^j$, in which two potentials $\tilde{\phi}^j(r,z,\omega)$ and $\tilde{\boldsymbol{\psi}}^j = [0,\, \tilde{\psi}^j(r,z,\omega),\, 0]^{\mathrm{T}}$ suffice for determining the wave field in each solid layer

$$\nabla^2 \tilde{\phi}^j(r,z,\omega) + k_{L,j}^2 \tilde{\phi}^j(r,z,\omega) = 0, \quad (5)$$

$$\nabla^2 \tilde{\psi}^j(r,z,\omega) - \frac{\tilde{\psi}(r,z,\omega)}{r^2} + k_{T,j}^2 \tilde{\psi}^j(r,z,\omega) = 0 \quad (6)$$

with $k_{L,j}^2 = \omega^2/c_{L,j}^2$ and $k_{T,j}^2 = \omega^2/c_{T,j}^2$, in which $c_{L,j}$ and $c_{T,j}$ denote the speeds of the compressional and shear waves in layer j, respectively. In addition, a set of boundary conditions at $z = 0$, $z = D$ and a set of interface conditions between the adjacent layers should be satisfied, together with the interface conditions at the shell surface:

$$\tilde{p}_f(r, z_0, \omega) = 0,\ r \geq R, \quad (7)$$

$$\tilde{\sigma}_{s,zz}^1(r, z_1, \omega) + \tilde{p}_f(r, z_1, \omega) = 0,\ r \geq R, \quad (8)$$

$$\tilde{\sigma}_{s,zr}^1(r, z_1, \omega) = 0,\ r \geq R, \quad (9)$$

$$\tilde{u}_{s,z}^1(r, z_1, \omega) - \tilde{u}_{f,z}(r, z_1, \omega) = 0,\ r \geq R, \quad (10)$$

$$\sigma_{s,zi}^{j+1}(r, z_j, \omega) - \sigma_{s,zi}^j(r, z_j, \omega) = 0, i = z, r, \quad (11)$$

$$\tilde{u}_{s,i}^{j+1}(r, z_j, \omega) - \tilde{u}_{s,i}^j(r, z_j, \omega) = 0, i = z, r, \quad (12)$$

$$\tilde{u}_{s,r}^n(r, D, \omega) = \tilde{u}_{s,z}^n(r, D, \omega) = 0, \quad (13)$$

$$\tilde{u}_{p,r}(z, \omega) - \tilde{u}_{f,r}(R, z, \omega) = 0, z_0 < z < z_1, \quad (14)$$

$$\tilde{u}_{p,i}(z, \omega) - \tilde{u}_{s,i}(R, z, \omega) = 0,\ i = z, r. \quad (15)$$

In Eqs.(10) and (14), $\tilde{u}_{f,z}(r,z,\omega)$ and $\tilde{u}_{f,r}(r,z,\omega)$ correspond to the vertical and radial displacement components of the fluid (velocities divided by (iω) in the frequency domain), respectively.

A modal decomposition is applied both for the shell structure and the acousto-elastic waveguide. The modal expansion of the shell structure is introduced as

$$\tilde{u}_{p,j}(z, \omega) = \sum_{m=1}^{\infty} A_m\, U_{jm}(z) \quad (16)$$

The index $j = z, r$ indicates the corresponding displacement component, $m = 1, 2, ..., \infty$ is the axial order and the vertical eigenfunctions $U_{jm}(z)$ satisfy the chosen boundary conditions at $z = 0, L$ (any boundary conditions are allowed in this context). The expressions for the displacement and stress field in the waveguide which inherently satisfy Eqs.(5)-(13) as well as the condition at $r \to \infty$ are:

$$\tilde{v}_{f,z}(r, z, \omega) = \sum_{p=1}^{\infty} C_p\, H_0^{(2)}(k_p r)\, \tilde{v}_{f,z,p}(z), \quad (17)$$

$$\tilde{v}_{f,r}(r, z, \omega) = \sum_{p=1}^{\infty} C_p\, H_1^{(2)}(k_p r)\, \tilde{v}_{f,r,p}(z), \quad (18)$$

$$\tilde{p}_f(r, z, \omega) = \sum_{p=1}^{\infty} C_p\, H_0^{(2)}(k_p r)\, \tilde{p}_{f,p}(z), \quad (19)$$

$$\tilde{u}_{s,z}(r, z, \omega) = \sum_{p=1}^{\infty} C_p\, H_0^{(2)}(k_p r)\, \tilde{u}_{s,z,p}(z), \quad (20)$$

$$\tilde{u}_{s,r}(r, z, \omega) = \sum_{p=1}^{\infty} C_p\, H_1^{(2)}(k_p r)\, \tilde{u}_{s,r,p}(z), \quad (21)$$

$$\tilde{\sigma}_{s,zz}(r, z, \omega) = \sum_{p=1}^{\infty} C_p\, H_0^{(2)}(k_p r)\, \tilde{\sigma}_{s,zz,p}(z), \quad (22)$$

$$\tilde{\sigma}_{s,zr}(r, z, \omega) = \sum_{p=1}^{\infty} C_p\, H_1^{(2)}(k_p r)\, \tilde{\sigma}_{s,zr,p}(z), \quad (23)$$

$$\begin{aligned} \tilde{\sigma}_{s,rr}(r, z, \omega) &= \sum_{p=1}^{\infty} C_p\, H_0^{(2)}(k_p r)\, \tilde{\sigma}_{s,rr,p}^{H_0}(z) \\ &+ \frac{1}{r} \sum_{p=1}^{\infty} C_p\, H_1^{(2)}(k_p r)\, \tilde{\sigma}_{s,rr,p}^{H_1}(z). \end{aligned} \quad (24)$$

The functions $H_0^{(2)}(k_p r)$ and $H_1^{(2)}(k_p r)$ are the Hankel functions of the second kind of the zeroth and first order, respectively. The vertical eigenfunctions in the summation terms above as well as the material constants are defined explicitly over the total thickness of the waveguide by introducing the z-dependence and therefore the subscript index j is omitted hereafter for simplicity. The term k_p denotes the horizontal wavenumber which is the solution of the dispersion equation formed by the set of equations (7)-(13). In Eqs.(16)-(24) the only unknowns are the coefficients of the modal expansions A_m and C_p. A system of infinite algebraic equations with respect to the unknown coefficients C_p can be obtained by an appropriate combination of Eqs.(14)-(15) and the use of Eq.(1) [7]:

$$\begin{aligned} \sum_{q=1}^{\infty} C_q \Bigg(& L_{qp} + k_q\, H_1^{(2)}(k_q R)\, \Gamma_q\, \delta_{qp} - \\ & - \sum_{m=1}^{\infty} \frac{R_{mq}\, Q_{mp}}{I_m} \Bigg) = \sum_{m=1}^{\infty} \frac{F_m\, Q_{mp}}{I_m} \end{aligned} \quad (25)$$

The coefficients of the shell structure are given by

$$A_m = \frac{F_m + \sum_{p=1}^{\infty} C_p \, R_{mp}}{I_m} \tag{26}$$

The terms L_{qp}, Γ_q, Q_{mp}, R_{mp}, F_m and I_m introduced in Eqs.(25) and (26) as well as their physical interpretation are discussed in Tsouvalas and Metrikine [7].

3. Structure-borne wave radiation due to pile driving

Results are presented hereafter with the marine sediment is modelled as a layered elastic medium with modified properties to account for water saturation based on the works of Hamilton [8] and Buckingham [9]. The soil sediment is divided into two layers namely, an upper layer of *fine sand* which overlies a layer compiled of a mixture of sand, clay and silt (Table I). The properties of the two layers are obtained from Tables IB and VIB and Figs.7 and 16 of Hamilton [8], taking into account the related work of Buckingham [9]. The values α_p and α_s shown in Table I denote the attenuation of the compressional and shear waves in each layer. The material and geometrical properties of the shell structure are defined as follows: $E = 210000$MPa, $\nu = 0.28$, $\rho = 7850$kgm^{-3}, $R = 2.7$m, $L = D = 58$m, $2h = 0.05$m, $z_0 = 8$m, $z_1 = 18$m and $z_2 = 33$m. In the solution of Eq.(25), the number of shell modes considered are 400, which is regarded as sufficient for the frequency range of interest. An impulsive force is applied at the head with a maximum amplitude of 120MN and a pulse duration of about 0.005s. This corresponds approximately to a hammer energy input of 1000kJ.

In Fig.2, the wave radiation into the soil and into the water column is shown at several time moments after the hammer impact. Due to the symmetry of the loading conditions and the geometry, only the r-z plane is shown in the figure, i.e. the response is cylindrically symmetric. The pressure distribution in the fluid region is shown in the upper part ($z \leq 23$m), whereas in the lower part ($z > 23$m) the norm of the particle velocity vector is depicted. The following general observations need to be mentioned:

i) The response in the fluid region consists of compressional waves (pressure wave fronts) with an inclination of about 16° to the vertical. This is in full agreement with results presented elsewhere [6, 10];

ii) The response in the soil region consists of both shear and compressional waves. In the upper soil layer, the compressional waves have a speed which is larger than the speed of the bulk waves in the water ($c_{L,1} > c_f$) and therefore a slightly larger inclination to the vertical is observed. Shear wavefronts are also formed with almost vertical polarisation due to the large contrast between the velocity of the compressional waves in the pile ($c_p \simeq 5400$ ms^{-1}) and the shear wave speeds in the soil ($c_T \leq 200$ ms^{-1}). At the interface between the two soil layers, the inclination of the shear fronts increases in the lower soil medium because $c_{T,1} < c_{T,2}$. The main difference with respect to the cases analysed in [7] is that in the present case, the compressional waves in the soil propagate with speeds that are comparable to the ones of the pressure waves in the fluid region. At the interface between the two solids, the wave field is distorted due to the difference in the shear wave speeds between the two media and the possible existence of *Stoneley* waves;

iii) Scholte waves are generated at the seabed-water interface. Their amplitudes decrease with increasing distance from the interface and with increasing range from the pile surface. Nevertheless, it should be pointed out that even at a distance of 20m from the pile surface, the pressure amplitudes induced by the Scholte wave in the fluid region and in the vicinity of the seabed level are of the order of 80 kPa in this particular case; a magnitude comparable to the one induced by the fluid body waves.

In contrast to the case of the impact hammer, vibratory hammers drive the pile into the soil in a different manner. The input force consists of low frequencies and is periodic. For the case analysed here, the main driving frequency is around 20Hz which is a typical driving frequency for offshore vibratory hammers. A small amount of energy in concentrated at a few super-harmonics of the fundamental frequency up to 100Hz. The magnitude of the input force is about 10^6N ($\sim$ 100 less amplitude compared to the impact hammer). The investigated time window is chosen such that the full radiation pattern is developed. The material and geometrical properties of the coupled system are already given in section 3.

The structure-borne wave radiation in the case of vibratory piling is shown in Fig.3 and has the following characteristics:

i) The wave field in the soil consists mainly of vertically polarised shear waves with cylindrical fronts which spread outwards from the vibrating pile with the shear wave velocity;

ii) The Scholte waves, which propagate parallel to the seabed-water interface, attenuate much less in comparison with the shear waves in the soil;

iii) The pressures in the fluid are localised close to the seabed. The typical Mach wave radiation pattern in the fluid region cannot be distinguished in this case;

iv) The pressures in the water region are significantly lower when compared to the ones generated by the impact hammer due to the smaller amplitude

Table I. Acousto-elastic waveguide consisting of three layers (from top to bottom): water column, fine-sand layer and a sand-clay-silt layer. Properties derived from Tables IB and VIB and Figs. 7 and 16 of Hamilton [8], taking into account the related work of Buckingham [9].

Layer	Depth m	ρ kgm^{-3}	c_L ms^{-1}	c_T ms^{-1}	α_p dBm^{-1}kHz^{-1}	α_s dBm^{-1}kHz^{-1}
Water	18	1023	1453	–	–	–
Fine sand	10	1900	1797	113	0.40	15.0
Sand-silt-clay	25	1780	1635	175	0.30	13.0

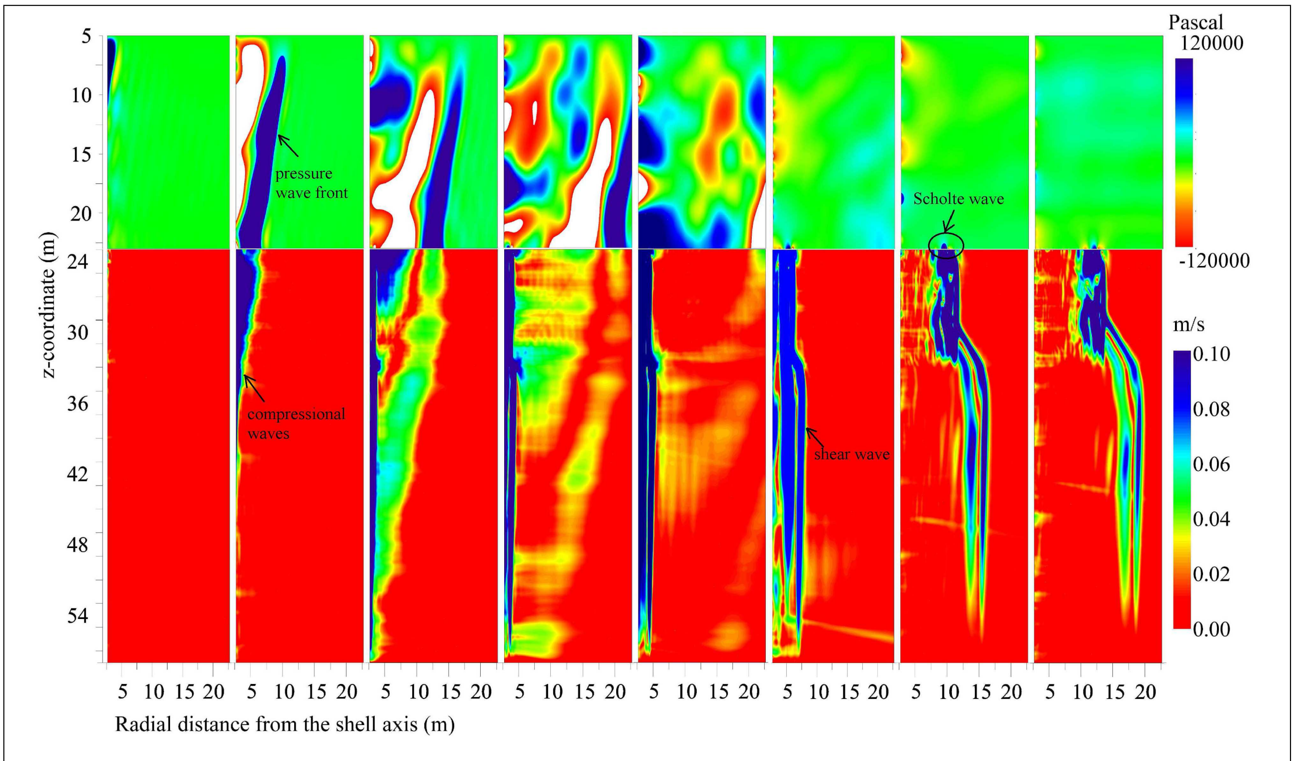

Figure 2. Pressures in the fluid ($z \leq 23$; top part of the figure) and velocity norm in the soil ($z > 23$; bottom part of the figure) for several moments in time after the hammer impact. From left to right the time moments are given in 10^{-3}s: $t = 8.4$; 13.2; 18; 22.8; 27.6; 42; 90; 108.

of the force and the inefficient sound radiation from the pile surface at frequencies below 100Hz. At this low frequency range only a few modes propagate in the water column, i.e. the majority of the energy irradiates into the soil domain.

The results regarding the wave radiation in the soil are in full agreement with the ones presented by Masoumi et al. [11], in which the vibrations of concrete piles subjected to a vibratory hammer excitation were examined.

4. CONCLUSIONS

In the present study, the wave radiation into the fluid-soil region caused by a steel monopile being driven into the soil offshore is analysed. The marine sediment is described as a layered elastic continuum with modified properties to account for water saturation. Thus, the co-existence of shear and compressional waves is allowed together with the associated interface modes. The modal decomposition method is applied for the solution of the problem. The dynamic response of each subsystem, i.e. the structural domain and the acousto-elastic waveguide, is expressed as an infinite set of eigenfunctions. The modal coefficients are then determined by an appropriate combination of the kinematic conditions at the interface of the two domains and the use of the orthogonality relations of each set of eigenmodes. Thus, the solution to the problem is semi-analytical and the only approximation employed is on the truncation of the modal expansions to reduce the infinite set of linear algebraic equations.

Results from impact pile driving show that the pressure field in the fluid consists mainly of conical fronts (*primary noise source*). In the soil region, both vertically polarised shear waves and compressional waves are generated, with the former being much stronger than the latter. In addition, Scholte waves are also present close to the seabed-water interface. They induce pressure fluctuations in the water column which

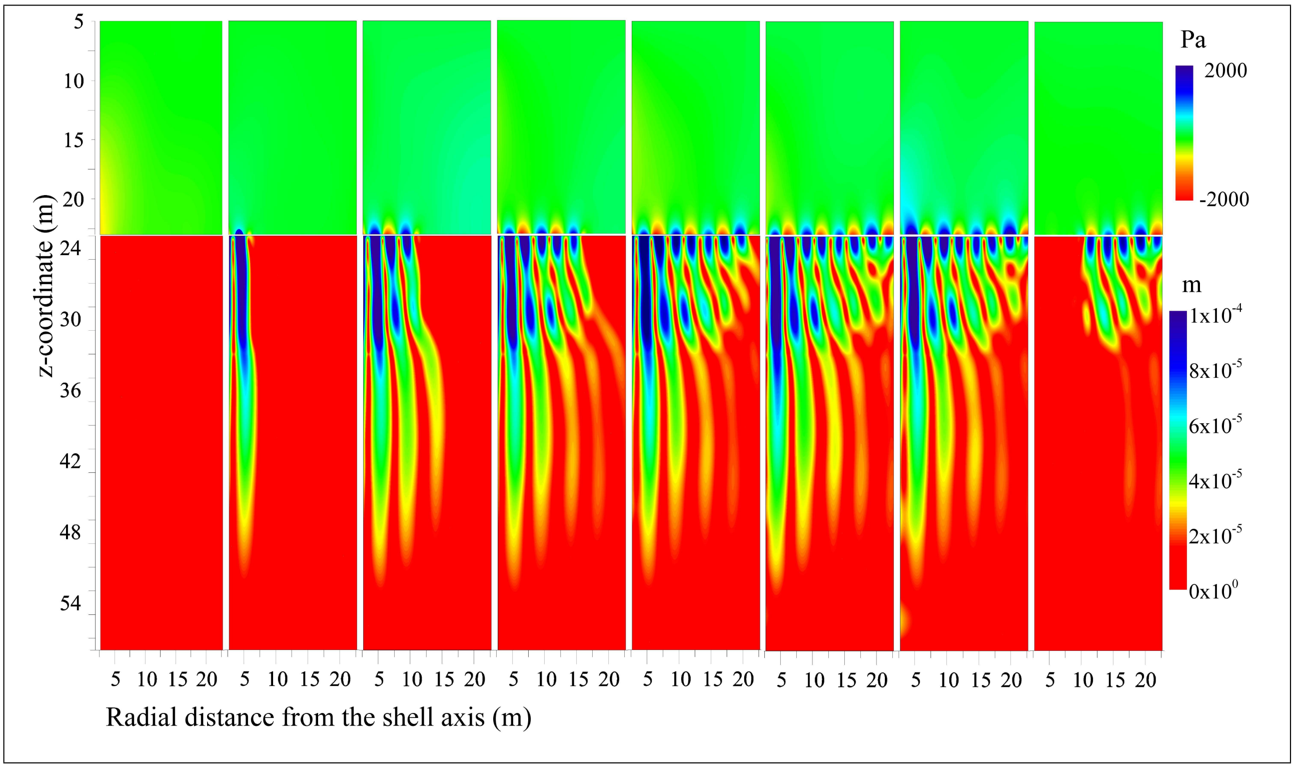

Figure 3. Pressures in the fluid ($z \leq 23$; top part of the figure) and displacement norm in the soil ($z > 23$; bottom part of the figure) for several moments in time for the case of installation with a vibratory device. From left to right the time moments are given in seconds: $t = 0.05$; 0.10; 0.15; 0.20; 0.25; 0.30; 0.50; 0.60.

can be of significant amplitude close to the seabed (*secondary noise path*). In the case of the vibratory hammer, the force contains a fundamental frequency together with several super-harmonics. The results show that the wave field in the soil consists of vertically polarised shear waves formed in cylindrical fronts and spreading outwards from the vibrating pile. *Scholte* waves are also generated close to the seabed-water interface. Their attenuation is much smaller in comparison with the shear waves in the soil. The pressures in the fluid are mainly localised close to the seabed, consist of low frequency components and are in general much lower than the ones obtained by the impact hammer.

Acknowledgement

This project has been funded by FLOW (Far and Large Offshore Wind Farms) in The Netherlands.

References

[1] H. Bailey, B. Senior, D. Simmons, J. Rusin, G. Picken, P. M. Thompson. Assessing underwater noise levels during pile-driving at an offshore windfarm and its potential effects on marine mammals. Marine Pollution Bulletin **60** (6), 888–897 (2010).

[2] C. Erbe. International regulation of underwater noise. Acoustics Australia **41** (1), 12–19 (2013).

[3] Joint Nature Conservation Committee (JNCC). Statutory nature conservation agency protocol for minimising the risk injury to marine mammals from piling noise. Aberdeen, UK (2010)

[4] S. Werner. Towards a precautionary approach for regulation of noise introduction in the marine environment from pile driving. Federal Environmental Agency, Stralsund (2010)

[5] E. McCarthy. International Regulation of Underwater Sound: Establishing Rules and Standards to Address Ocean Noise Pollution. Solid Mechanics and Its Applications Series, Springer (2004).

[6] A. Tsouvalas, A.V. Metrikine. A semi-analytical model for the prediction of underwater noise from offshore pile driving. Journal of Sound and Vibration **332** (13), 3232–3257 (2013).

[7] A. Tsouvalas, A.V. Metrikine. A three-dimensional vibroacoustic model for the prediction of underwater noise from offshore pile driving. Journal of Sound and Vibration **333** (8), 2283 – 2311 (2014).

[8] E. L. Hamilton. Geoacoustic modeling of the sea floor. J. Acoust. Soc. Am. **68** (5), 1313–1340 (1980).

[9] M. J. Buckingham. Compressional and shear wave properties of marine sediments: Comparisons between theory and data. J. Acoust. Soc. Am. **117** (1), 137–152 (2005).

[10] P. G. Reinhall, P. H. Dahl. Underwater mach wave radiation from impact pile driving: Theory and observation. J. Acoust. Soc. Am. **130** (3), 1209–1216 (2011).

[11] H.R. Masoumi, G. Degrande. Numerical modelling of free field vibrations due to pile driving using a dynamic soil-structure interaction formulation, Journal of Computational and Applied Mathematics (2008), 503-511.